Identical Linkage and Cooperativity of Oxygen and Carbon Monoxide Binding to *Octopus dofleini* Hemocyanin†

Patrick R. Connelly,‡ Stanley J. Gill,*,‡ Karen I. Miller,§ G. Zhou,§ and K. E. van Holde§

Department of Chemistry and Biochemistry, University of Colorado, Boulder, Colorado 80309-0215, and Department of Biochemistry and Biophysics, Oregon State University, Corvallis, Oregon 97331

Received July 12, 1988; Revised Manuscript Received September 30, 1988

ABSTRACT: Employment of high-precision thin-layer methods has enabled detailed functional characterization of oxygen and carbon monoxide binding for (1) the fully assembled form with 70 binding sites and (2) the isolated chains with 7 binding sites of *Octopus dofleini* hemocyanin. The striking difference in the cooperativities of the two ligands for the assembled decamer is revealed through an examination of the binding capacities and the partition coefficient, determined as functions of the activities of both ligands. A global analysis of the data sets supported a two-state allosteric model assuming an allosteric unit of 7. Higher level allosteric interactions were not indicated. This contrasts to results obtained for arthropod hemocyanins. Oxygen and carbon monoxide experiments performed on the isolated subunit chain confirmed the presence of functional heterogeneity reported previously [Miller, K. (1985) *Biochemistry 24*, 4582–4586]. The analysis shows two types of binding sites in the ratio of 4:3.

Hemocyanins are large multisubunit proteins that provide oxygen transport in many species of arthropods and molluscs. Arthropod hemocyanins contain one oxygen binding site per subunit (Miller & Van Holde, 1982), and native arthropod structures contain hexameric arrangements of subunits. The number of hexamers assembled to form the functional macromolecule varies among species and ranges from 1 to 8. On the other hand, molluscan hemocyanins are composed of 10 or 20 subunits, arranged to form hollow cylinders (Miller & Van Holde, 1982), each subunit having seven or eight oxygen binding sites. Despite the differences in the gross structural anatomy of these two types of hemocyanin molecules, they bear strong similarities in their functional chemistry. Both bind oxygen in a highly cooperative manner, and both show a strong Bohr effect.

In contrast to oxygen binding, carbon monoxide binds to hemocyanins noncooperatively, or with only slight positive cooperativity, and does not exhibit an appreciable Bohr effect (Bonaventura et al., 1974; Brunori et al., 1981; Richey et al., 1985). This marked difference in oxygen and carbon monoxide binding makes these ligands useful probes for the functional energetics of hemocyanin. Furthermore, carbon monoxide and oxygen bind to the same binuclear copper site of the protein in a mutually exclusive manner, with identical stoichiometry. This type of competitive, functional linkage, termed *identical linkage* (Wyman, 1948), leads to a simplified quantitative description of the liganded species. Studying the simultaneous binding of the two ligands to several species of arthropod hemocyanins has given insight into the cooperative binding mechanism, explained in terms of two levels of allosteric interaction within these multisubunit macromolecules (Robert et al., 1987; Richey et al., 1985; Decker et al., 1986, 1988). In the present study we have applied this approach to explore the functional chemistry of the large multisubunit molluscan hemocyanin from *Octopus dofleini*.

The structure of *O. dofleini* hemocyanin is among the simplest and best characterized of the molluscan hemocyanins (Miller, 1985; Lamy et al., 1987). It contains seven binding sites per subunit chain, and unlike many other molluscan hemocyanins, only a single type of subunit chain makes up the native decameric structure. Among the properties that are determined in this study and that serve to characterize the functional chemistry of the hemocyanin molecule are the binding capacities and linkage derivatives of oxygen and carbon monoxide and the CO/O_2 partition coefficient (Wyman, 1984). By considering these functional properties within the framework of a mechanistic model, we find that the combined use of CO and O_2 provides a basis for a simple picture relating structural and functional aspects of a large multisite molluscan protein.

Materials and Methods

Materials. Purification of *O. dofleini* hemocyanin was carried out as described previously (Miller, 1985). The concentration of protein used for the binding studies on the decameric form of the protein was 40 mg/mL as calculated from the extinction coefficient at 280 nm, $\epsilon = 1.394$ mg^{-1} cm^2 (Miller et al., 1988). The solution conditions used included the components of a physiological saline described by Miller (1985), which include the major ions present in *Octopus* blood (Potts & Todd, 1965). All solutions used for the studies of the decameric form were buffered with 0.1 M Hepes [*N*-2-hydroxyethyl)piperazine-*N*′-2-ethanesulfonic acid]. Experiments were performed at two values of pH, 7.25 and 7.60, chosen since under these conditions oxygen binding was high and moderate, respectively (Miller, 1985). The temperature of the solutions was kept constant at 25 °C with a water bath regulated by a Tronac Model PTC-40 precision temperature controller. To ensure that ligand-induced dissociation of the protein was negligible under our solution conditions, additional O_2 binding experiments were performed with the same sample diluted 1:5 with buffer. The binding curves for the two concentrations were essentially identical. Previous studies with an analytical ultracentrifuge (Van Holde & Miller, 1985)

† This work was supported by National Institutes of Health Grant HL22325 (S.J.G.) and National Science Foundation Grant DMB8510310 (K.I.M. and K.E.v.H.).

‡ University of Colorado.

§ Oregon State University.

0006-2960/89/0428-1835$01.50/0

confirm that the decamer is the stable species under the solution conditions used in this study.

Isolated chains of hemocyanin were prepared by dialyzing against 0.1 M tris(hydroxymethyl)aminomethane with 10 mM EDTA at pH 8.0 and then redialyzing against the same buffer at pH 8.0 without EDTA (Miller, 1985). The final concentration of hemocyanin was 8 mg/mL as determined from the extinction coefficient for isolated subunit chains at 280 nm, $\epsilon = 1.356$ mg^{-1} cm^2 (Miller et al., 1988). Binding curves were performed at 25 °C.

Binding Curve Measurement. The binding curves were obtained with the thin-layer optical absorbance cell described previously (Dolman & Gill, 1978). Four types of experiments were performed. Pure O_2 and CO binding curves were obtained by equilibrating the thin layer of hemocyanin with wet O_2 or CO at atmospheric pressure and then diluting the gas phase in contact with the solution with N_2. The presence of bound O_2 was monitored by the absorbance change at 345 nm and that of bound CO monitored by the absorbance change at 315 nm (Bonaventura et al., 1974) with a Cary 219 spectrophotometer.

In a third type of experiment, the hemocyanin solution was saturated with O_2, and then dilutions with CO were made to follow the competitive replacement binding reaction. In this experiment the sum of the partial pressures of oxygen and carbon monoxide remains constant. The fourth type of experiment was carried out by equilibrating the protein solution with a mixture of CO and O_2 to known partial pressures. Dilutions of this mixture were made with N_2 such that the ratio of partial pressures of CO and O_2 remained constant. The bound O_2 was monitored in these experiments by following the absorbance change at 345 nm, where there is no contribution to the spectral signal from the CO–protein complex. The remarkable stability of the thin layers of solution permitted more than one type of experiment to be performed with the same layer, since the base-line absorbance of the thin layer remained stable for at least 12 h. The combination of all four types of experiments allowed us to study the hemocyanin in its various stages of ligation with the two gaseous ligands. Further details of these procedures have been discussed elsewhere (Zolla et al., 1985; DiCera et al., 1987a).

Data Analysis. At each dilution step in an experiment, the absorbance change is computed. The observed change in absorbance for the ith dilution step where the ligand partial pressure changes from x_{i-1} to x_i is given by

$$\Delta A_i = \Delta A_T(\theta_i - \theta_{i-1}) \quad (1)$$

where θ is the extent of the reaction process at a given step and ΔA_T is a fitted parameter corresponding to the asymptotic absorbance change between the two extreme states (i.e., states where $\theta = 0$ and $\theta = 1$) of the hemocyanin molecule in a particular experiment. For example, in the pure oxygen titration experiment, ΔA_T is the difference in the absorbance between fully oxygenated and fully deoxygenated sample.

For the case of pure oxygen binding, the continuous representation of the function given in eq 1 is obtained by writing $x_{i-1} = x_i/D$, where D is the dilution factor for the thin-layer device (in these experiments $D = 0.6951$), and the resulting ΔA values are positioned at the arithmatic mean of the Δ log $p(O_2)$ interval. The oxygen partial pressure at this point, ξ, is then given by the geometric mean of the initial and final pressures, i.e., $\xi_i = (x_i x_{i-1})^{1/2}$. In this way, the plotted function is proportional to the oxygen binding capacity (DiCera et al., 1987b) of the hemocyanin expressed in terms of finite differences. Similar reasoning leads to the function for the pure carbon monoxide binding capacity.

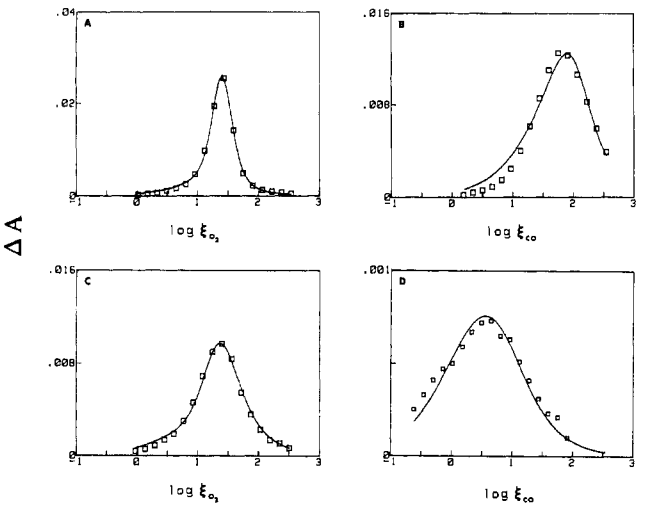

FIGURE 1: Derivative binding data for the experiments outlined under Materials and Methods at pH 7.25: (A) O_2 binding, (B) replacement of O_2 by CO, (C) displacement of ligands at a constant ratio of O_2 to CO activities (=552.59/46.96), and (D) CO binding. Each plot records the changes in absorbance corresponding to the changes in ligand partial pressure. The titration points in each of the plots are positioned at the mean of the logarithms of the initial and final partial pressures of oxygen (panels A and C) or carbon monoxide (panels B and D) for each titration step (log ξ). The theoretical curves are thus finite difference derivatives of the binding curves and represent the best fit upon simultaneously fitting the data sets with the model given in eq 2. The standard error of a point for the simultaneous fit is 4.2×10^{-4} absorbance.

All binding parameters as well as the ΔA_T's were estimated by least-squares regression analysis using the Gauss–Newton algorithm as modified by Marquardt (Bevington, 1969).

Results

Analysis of Oxygen and Carbon Monoxide Binding to the Decameric Form. Binding data for the four types of experiments outlined under Materials and Methods are shown in Figure 1 in the form of derivative binding curves. These plots represent the observed change in absorbance versus the logarithm of the geometric mean of the initial and final partial pressures of either CO or O_2 for each step. For the decameric form of *Octopus* hemocyanin, containing 70 binding sites for either CO or O_2, a phenomenological description of the equilibria is represented by reactions between the possible ligated species as depicted in Figure 2, where M is the unligated species, X represents O_2, and Y represents CO. The value of t (specified as t_D for the *Octopus* hemocyanin decamer) is 70. The general reaction of forming MX_iY_j is $M + iX + jY \rightarrow MX_iY_j$. In this array there are $(t + 1)(t + 2)/2$ species and therefore one less of this number of independent reactions. For the decamer there are 2556 species and 2555 reactions. Clearly it is impractical to analyze data in this way.

By turning to a simplified, allosteric description of the system, one is able to provide a tractable quantitative description of the binding process in terms of structural features of the multisubunit complex. The simplest allosteric description that accounts for the cooperative binding behavior is the two-state allosteric model—the so-called MWC model (Monod et al., 1965). Higher levels of allosteric interaction can be formulated in nested models (Robert et al., 1987). A fundamental quantity, which serves as a quantitative expression of the physical picture embodied by any model, is the binding polynomial (Wyman, 1964). From the binding polynomial, the necessary thermodynamic parameters may be derived.

For the *O. dofleini* hemocyanin decamer, a first-level MWC binding polynomial expression which takes into account the

Table I: Binding Parameters and Partition for O_2 and CO Binding to *Octopus* Hemocyanin

decamer[a]			subunit[b]	
binding parameter[c]	pH 7.25	pH 7.60	binding parameter	pH 8.00
κ_{Rx}	0.19 ± 0.054	0.23 ± 0.036	κ_{1x}	0.014 ± 0.002
κ_{Ry}	1.1 ± 0.3	0.46 ± 0.068	κ_{1y}	0.29 ± 0.05
κ_{Tx}	0.010 ± 0.001	0.076 ± 0.010	κ_{2x}	0.09 ± 0.01
κ_{Ty}	0.21 ± 0.014	0.23 ± 0.021	κ_{2y}	0.12 ± 0.01
log L	5.4 ± 0.72	1.8 ± 0.32		
m_R	5.8	2.0	m_1	21
m_T	21	3.0	m_2	1.3

[a] Solution conditions: 0.1 M Hepes buffer (see Materials and Methods) at 25 °C. [b] Solution conditions: 0.1 M Tris buffer (see Materials and Methods) at 25 °C. [c] The binding constants in units of $Torr^{-1}$ were determined by simultaneous fit of all of the experiments discussed in the text. The errors on the parameters are twice the value of the errors estimated in the fit. Partitions coefficients, m's, for each allosteric state of the decamer and each site type of the subunit are calculated from best fit parameters.

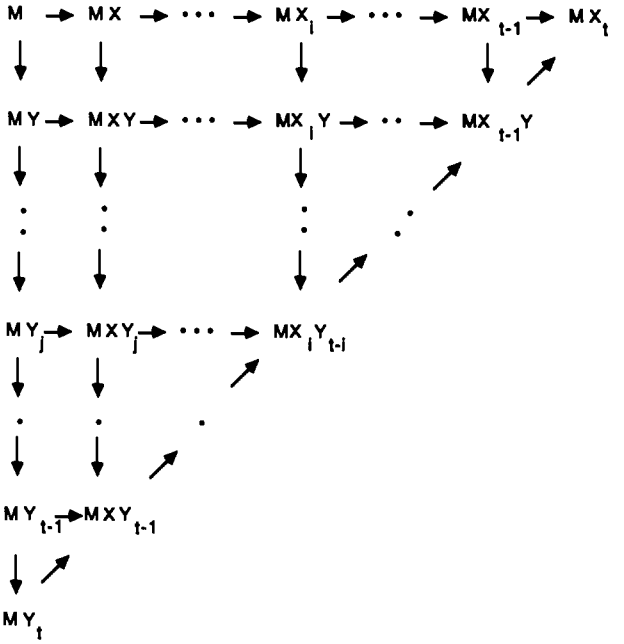

FIGURE 2: Species array for an identically linked system having t sites for either ligand, M, X, and Y represent the macromolecule, oxygen, and carbon monoxide, respectively. The array is triangular since no more than a total of t ligands, regardless of type, may be bound simultaneously.

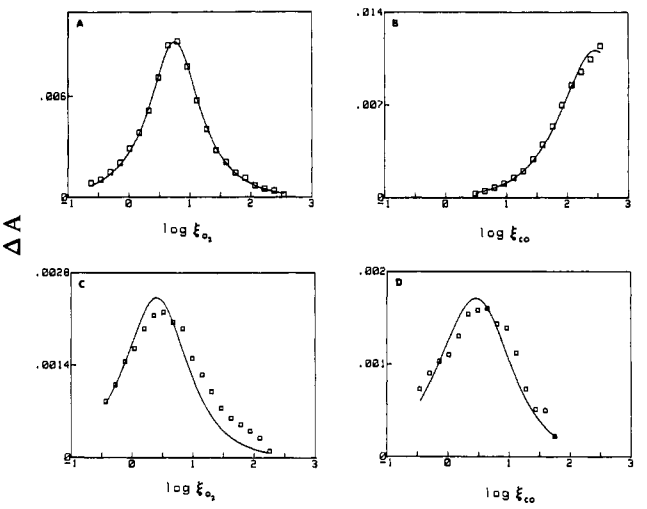

FIGURE 3: Derivative binding data for the experiments outlined under Materials and Methods at pH 7.6: (A) O_2 binding, (B) replacement of O_2 by CO, (C) displacement of ligands at a constant ratio of O_2 to CO activities (=309.74/289.40), and (D) CO binding. Each plot records the changes in absorbance corresponding to the changes in ligand partial pressure. The titration points in each of the plots are positioned at the arithmatic mean of the logarithms of the initial and final partial pressures of oxygen (panels A and C) or carbon monoxide (panels B and D) for each titration step (log ξ). The standard error of a point for the simultaneous fit is 2.1×10^{-4} absorbance.

identically linked nature of oxygen and carbon monoxide binding is

$$P_{xy}(\text{decamer}) = [(1 + \kappa_{Rx}x + \kappa_{Ry}y)^n + (1 + \kappa_{Tx}x + \kappa_{Ty}y)^n]^{t_D/n} \quad (2)$$

In this equation, the κ's are the association constants for oxygen or carbon monoxide binding to one of the two allosteric forms of the macromolecule (R and T), n is the number of binding sites in the allosteric unit, and x and y are the activities of oxygen and carbon monoxide. The contribution of each allosteric unit is given by the bracketed terms. Assuming each allosteric unit functions independently, the complete binding polynomial is simply given by the product of each term; i.e., one term is raised to the power of the number of allosteric units given by t_D/n. The amounts of oxygen and carbon monoxide bound are given by the derivative of the logarithm of the binding polynomial with respect to the logarithm of the activities of oxygen and carbon monoxide, respectively (Wyman, 1964). The theoretical curves in Figure 1 represent the best fit to the data based upon $n = 7$ and $t_D/n = 10$. Other choices gave an inferior fit.

All five binding parameters of the allosteric model, as well as the total absorbance changes for each derivative binding curve, were allowed to vary freely in the simultaneous fit of the four data sets of Figure 1. For practical purposes, we used the logarithm of L as a fitting parameter since this led to a more rapid convergence. Repeat experiments on the same sample preparation (data not shown) gave parameters within the confidence intervals reported in Table I, determined from the asymptotic covariance matrix (Ratkowsky, 1985). The same series of experiments was performed at pH 7.60, where the oxygen binding curve had a different shape and symmetry than that at pH 7.25. The two-state model adequately described these data also (Figure 3, Table I).

Resolution of the binding constants of oxygen and carbon monoxide to each allosteric state depends on the populations of the states with the ligands bound. When the pure oxygen data set were fitted alone, resolution of each of the model binding parameters could be achieved. Carbon monoxide, however, does not promote a strong shift in the populations of the allosteric states upon binding. Furthermore, the affinities of the ligands for each state are not greatly different. When the pure carbon monoxide binding data were fitted alone, the values of the binding constant to the R state could not be resolved, nor could the value of L. The experiments in which both gases were present (Figures 1 and 3, panels B and C) permit one to probe both allosteric states with carbon

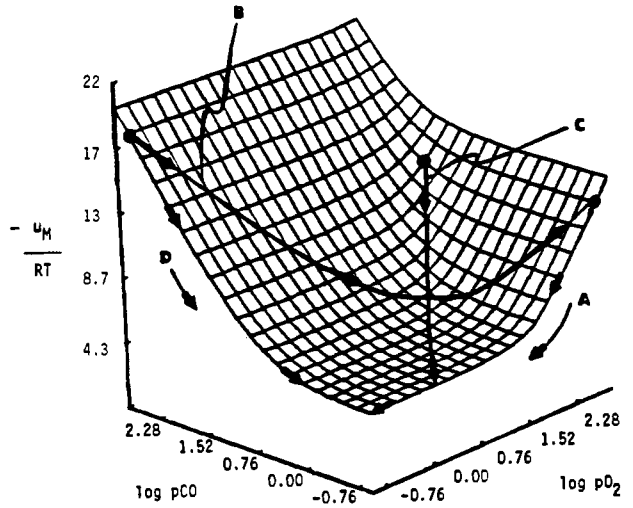

FIGURE 4: Chemical potential of the macromolecule ($-\mu_M = RT \ln P_{xy}$), plotted as a function of the logarithms of oxygen and carbon monoxide activities, revealing the states probed by the various experiments described under Materials and Methods: (A) pure oxygen experiment, (B) competitive displacement of carbon monoxide by oxygen, (C) displacement of both ligands with activities held at a fixed ratio, and (D) pure carbon monoxide experiment. The curvature of the surface along a specific path is related to the measurements depicted in Figures 1 and 3, as described in the text.

monoxide bound, and therefore resolution of all binding parameters upon simultaneously fitting the data from all four types of experiments.

The number of protons released on oxygen binding was estimated from the constants reported in Table I. For pure oxygen binding the proton release is 1.7 mol of H^+/mol of oxygen bound, in agreement with the results reported by Miller (1985) at 10 and 20 °C, which show virtually no temperature dependence of the Bohr effect. For the replacement of carbon monoxide by oxygen the proton release is 1.6 mol of H^+/mol of oxygen bound. Carbon monoxide does not promote any appreciable proton release.

Thermodynamic Surfaces for O_2 and CO Binding to the Decamer. In order to compare the binding properties of CO and O_2 and reveal the information given by the various experiments that were used to determine the relevant properties of the ligands for the macromolecule, it is useful to consider a three-dimensional representation of the chemical potential of the macromolecule in terms of coordinates proportional to the chemical potentials of the two ligands. The result shown in Figure 4 was generated from the binding polynomial for the data collected at pH 7.25. The slope of this surface parallel to the chemical potential of oxygen at constant carbon monoxide chemical potential gives the amount of oxygen bound at a point on the surface (Wyman, 1984). The amount of carbon monoxide bound is given by the slope along the carbon monoxide coordinate at the same point. The edges of the surface parallel to the ligand chemical potentials were probed in the pure oxygen and carbon monoxide experiments. Other paths on this surface were followed in the mixed gas experiments, allowing the macromolecule to be studied with both types of ligands bound simultaneously.

The actual experimental quantities that are measured are related to the second derivatives, i.e., the curvature of the surface shown in Figure 4. Two of these quantities are the homotropic derivatives, termed binding capacities (DiCera et al., 1987b). They are a measure of the way in which the amount of a ligand bound changes upon changing the partial pressure of that ligand. Figures 5 and 6 depict the binding capacity surfaces for carbon monoxide and oxygen, respec-

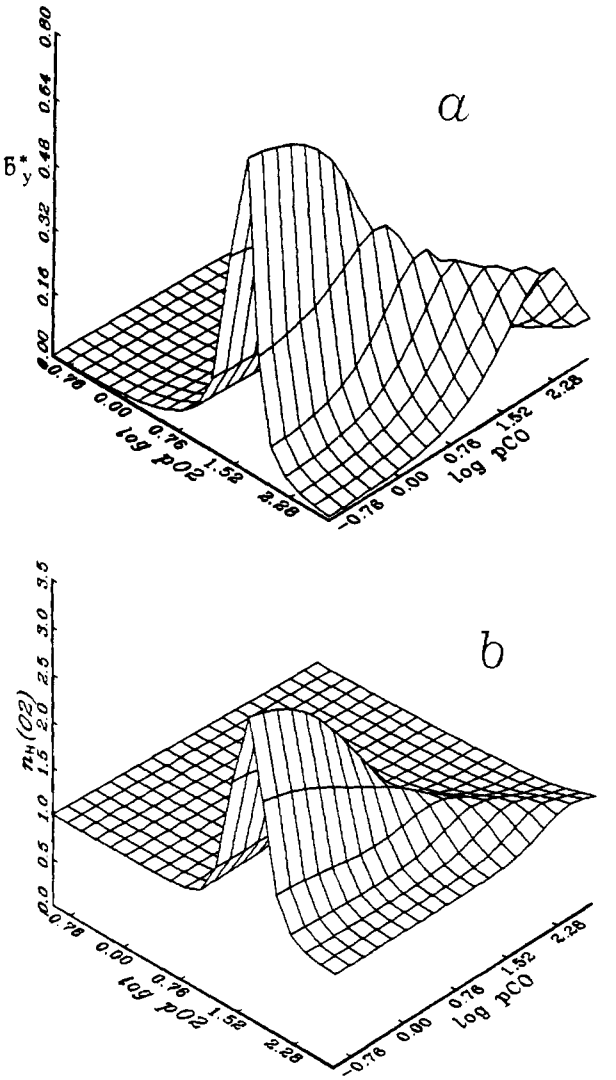

FIGURE 5: Reduced oxygen binding capacity (a) and Hill slope (b) surfaces for *O. dofleini* hemocyanin at pH 7.25. Each of these figures describes the cooperativity of oxygen binding as a function of the logarithm of the activities of CO and O_2. The oxygen binding capacity is the curvature of the surface along the log $p(O_2)$ axis shown in Figure 4.

tively, normalized to the number of binding sites and RT. The reduced binding capacities are denoted by $\mathbb{B}^*_y$ and $\mathbb{B}^*_x$ for oxygen and carbon monoxide and are given by $\mathbb{B}^*_y \equiv t^{-1}(\partial \bar{X}/\partial \ln x)_y$ and $\mathbb{B}^*_x \equiv t^{-1}(\partial \bar{Y}/\partial \ln y)_x$, where $\bar{X}$ and $\bar{Y}$ denote the amounts of X and Y bound per mole of macromolecule and t is the number of binding sites.[1] The sharpness of the oxygen binding capacity surface is a clear demonstration of the cooperativity exhibited in the oxygen binding process. A third quantity is revealed through the reduced heterotropic linkage derivative [$\Gamma^*_x \equiv t^{-1}(\partial \bar{X}/\partial \ln y)_x = \Gamma^*_y \equiv t^{-1}(\partial \bar{Y}/\partial \ln x)_y$], which describes the linkage between the two ligands. It is described geometrically by the way the slope of the macromolecular chemical potential surface in one direction changes with variation in the other direction. Figure 7 depicts the

[1] The notation used here for the *reduced* binding capacity (denoted by an asterisk) recognizes the usual convention of the subscript denoting fixed conditions as for heat capacity at constant pressure. The reduced and normal binding capacities are related by $\mathbb{B}^*_y = (RT/t)\mathbb{B}_y$. This is a convenient addition to the original notation (DiCera et al., 1987b). The symbol B is used in this paper in place of the Russian B chosen in the original definition (Di Cera et al., 1988b), since the Russian B is not one of the characters available to this Journal.

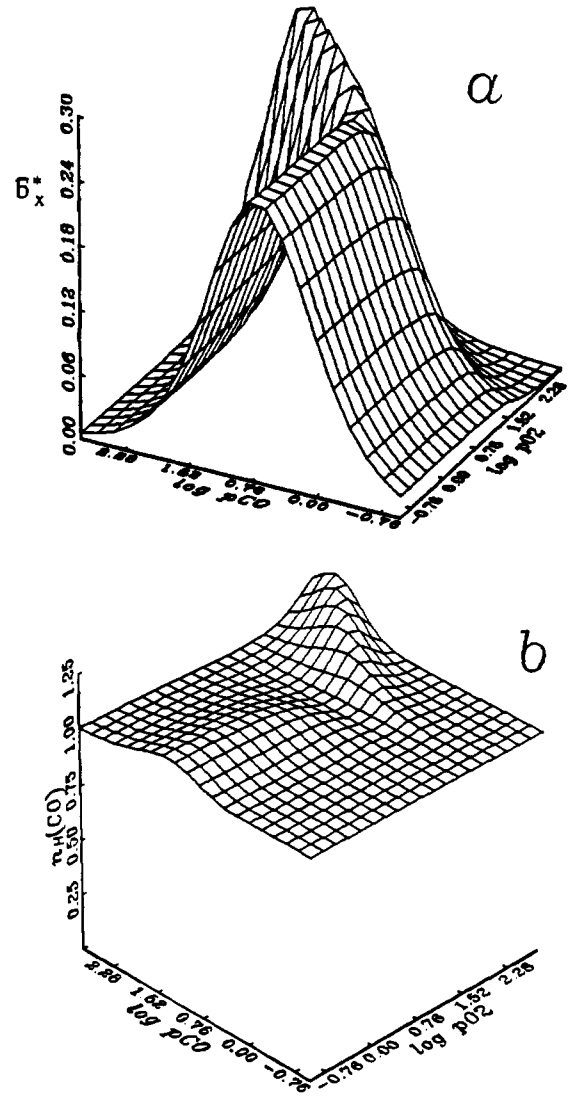

FIGURE 6: Reduced carbon monoxide binding capacity (a) and Hill slope (b) surfaces for *O. dofleini* hemocyanin. CO binding is nearly noncooperative in the absence of oxygen, but a definite positive cooperativity is present at high oxygen partial pressure.

surface describing this linkage property. In the experiments that involve mixtures of both ligands, a combination of the binding capacities and the heterotropic linkage quantity is measured. More specifically, in the experiment in which the ratio of ligand activities is held constant, the measured derivative is the sum of the oxygen binding capacity and the linkage property, the sum of the curvatures in each direction parallel to the axes at a point along the path labeled C in the macromolecular chemical potential surface, i.e., $\Gamma^*_y + B^*_y$. In the experiment that tracks along the path labeled B in the same surface, a weighted sum of the curvatures in each direction is measured, i.e., $\Gamma^*_y - (y/x)B^*_y$.

The classical way to describe the differences in the binding of oxygen and carbon monoxide is to calculate the partition coefficient, m, defined as the ratio of carbon monoxide to oxygen bound times x/y (Haldane & Smith, 1897; Wyman, 1948). In the case that both ligands bind with the same cooperativity, this surface would be a plane and takes on a constant value at all levels of ligand saturation. The drastic nonuniformity in the partition coefficient plot (Figure 8) further enphasizes the differences in the cooperative binding properties of the two ligands.

Analysis of Oxygen and Carbon Monoxide Binding to the Isolated Subunits. Since the isolated chain of *Octopus* he-

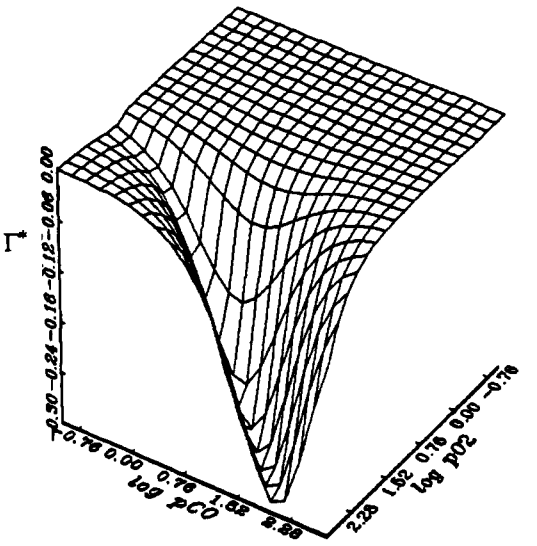

FIGURE 7: Linkage between oxygen and carbon monoxide binding given by the reduced heterotropic derivative of the macromolecular chemical potential. The competitive binding interaction results in the negative values which the heterotropic property produces.

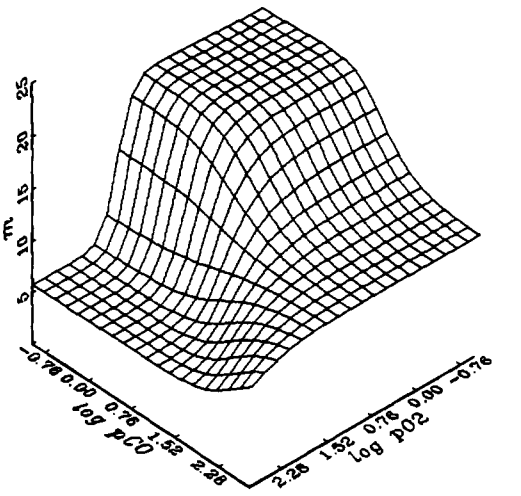

FIGURE 8: Partition coefficient (m) of oxygen and carbon monoxide at pH 7.2. The drop in partition coefficient at high ligand activities reflects the change in the partition coefficients for the two allosteric states whose populations are shifted upon ligation. At low partial pressures of both ligands, the macromolecule is in the T state, having a partition coefficient of 21 (see Table I). At high partial pressure of oxygen and low partial pressure of carbon monoxide, the macromolecule is largely in the R state, and thus m assumes a value close to m_R (5.8).

mocyanin contains seven binding sites, it is possible that cooperative binding can occur. However, Miller (1985) demonstrated that oxygen binding to the isolated chains produces Hill slopes of less than 1, suggesting the presence or more than one type of binding site within the subunit. By performing the analysis of oxygen and carbon monoxide data from experiments similar to those performed on the decamer, it is possible to obtain the affinities and relative numbers of the different types of sites within the chain (Zolla et al., 1985). Figure 9 shows the data for the experiments performed on the isolated subunit chain. Pure carbon monoxide binding curves were not performed owing to the small difference in the absorbance between unliganded and carbonmonoxygenated hemocyanin at the protein concentration used. The analysis does require this experiment to resolve the binding parameters.

The theoretical curves in Figure 9 were developed from the expression for the binding polynomial for the isolated subunit.

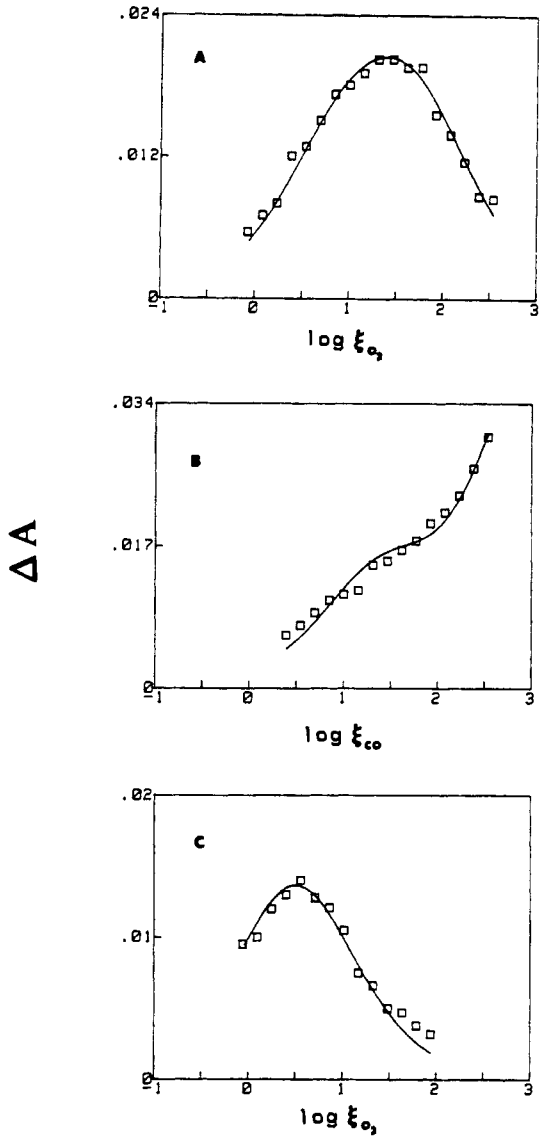

FIGURE 9: Derivative binding data for isolated subunits: (A) O_2 binding, (B) replacement of O_2 by CO, and (C) displacement of ligands at a constant ratio of O_2 to CO activities (=148.737/144.664) at pH 8.0. Each plot records the changes in absorbance corresponding to the changes in ligand partial pressure. The titration points in each of the plots are positioned at the arithmetic mean of the logarithms of the initial and final partial pressures of oxygen (panels A and C) and carbon monoxide (panel B) for each titration step (log ξ). The standard error of a point for the simultaneous fit is 0.9×10^{-4} absorbance.

The most simple departure from a simple independent site binding model that incorporates the feature of site heterogeneity is a model that assumes two types of binding sites. The appropriate expression for the binding polynomial relevant to O_2 and CO binding to isolated *Octopus* hemocyanin chains is

$$P_{xy}(\text{chain}) = (1 + \kappa_{1x}x + \kappa_{1y}y)^{w}(1 + \kappa_{2x}x + \kappa_{2y}y)^{t-w} \quad (3)$$

The κ's are the association constants of oxygen or carbon monoxide to the two different types of sites, type 1 and type 2, of the chain, and w and $t - w$ are the numbers of sites having affinities of types 1 and 2, respectively. The value of t for the isolated chain is $t_c = 7$. The constants that were obtained upon fitting the data in Figure 9 simultaneously are reported in Table I.

To facilitate a comparison of the binding properties of the isolated chain and decamer, surface plots of the binding capacities and linkage derivatives for the isolated chains are shown in Figure 10.

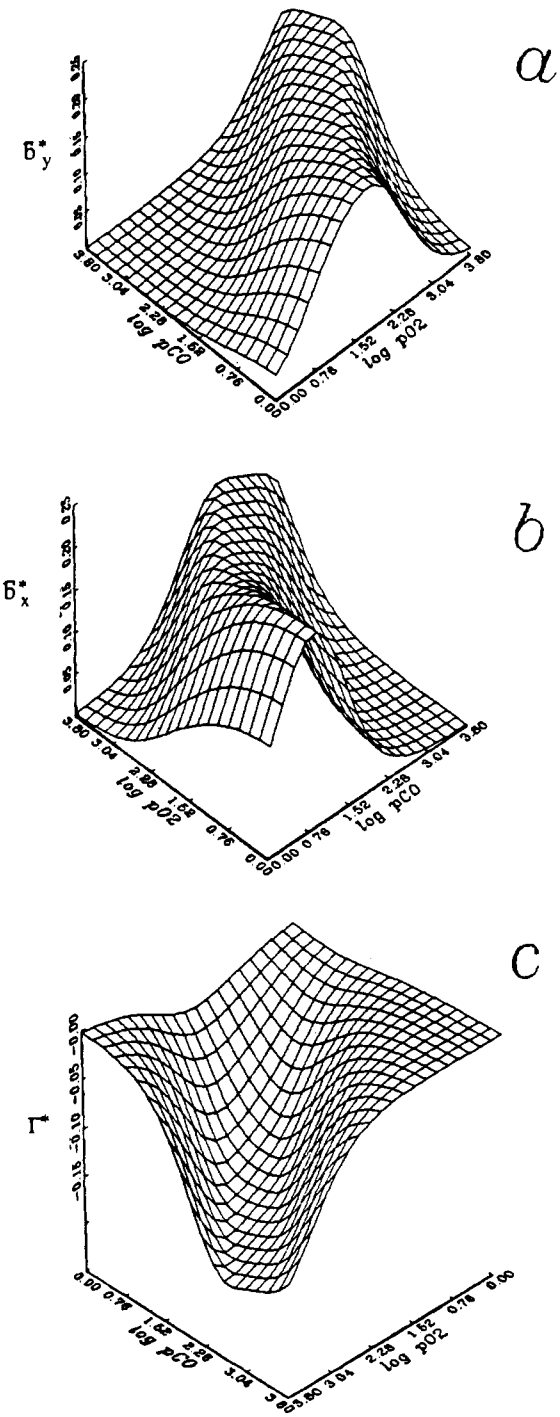

FIGURE 10: Thermodynamic surfaces describing the oxygen and carbon monoxide binding to isolated subunits of *O. dofleini*: (a) reduced oxygen binding capacity; (b) reduced carbon monoxide binding capacity; (c) reduced heterotropic linkage property surface.

Discussion

Model for Oxygen and Carbon Monoxide Binding to the Decamer. Although the binding of a single type of ligand to a macromolecule is useful in assessing the functional properties of a system, deeper insight is provided by an examination of the binding of more than one type of ligand. In the case of respiratory proteins one often looks to the proton as an additional ligand because of its physiological significance as a regulator of oxygen binding. However, the large number of proton binding sites makes it difficult to carry out a detailed

analysis of proton binding in terms of specific site properties. Because CO and O_2 bind competitively to a defined set of sites, it becomes feasible to determine their binding reactions in detail. Carbon monoxide is a particularly convenient ligand to study. The stoichiometry of the CO–hemocyanin complex is known. The amount of bound carbon monoxide is easily measured by a spectroscopic signal at 315 nm (Bonaventura et al., 1974), and since carbon monoxide is a gaseous ligand, activity can be controlled to high precision. The dramatic differences in the functional chemistry that CO and O_2 exhibit raise key questions about the molecular details of cooperativity.

The simplifying features in the analysis and acquisition of precise binding data on both oxygen and carbon monoxide binding facilitate testing of a particular molecular model for the binding behavior. This was realized in the case of lobster hemocyanin in which the oxygen binding data could be described by a simple two-state MWC model, but the carbon monoxide and competitive binding data showed that the MWC model was inconsistent (Richey et al., 1985). Miller (1985) reported pure oxygen binding curves of *Octopus* hemocyanin at a series of pH's and found the MWC model to be sufficient to represent the data. For the *Octopus* hemocyanin, by analyzing the binding of pure oxygen and carbon monoxide along with competitive binding of these ligands, we find a good fit to the simple allosteric model outlined above.

Two criteria for determining the applicability of the allosteric model described by the binding polynomial given in eq 2 are as follows: (1) the value of n (the number of sites in the allosteric unit) obtained upon fitting the binding data, or the value of n that is fixed to a selected value in the fitting procedure, should correspond to a physically reasonable structural unit of the molecule; and (2) the value of t_D/n must be an integer corresponding to the structural features of the composite macromolecule. In the case of tarantula hemocyanin, an arthropod hemocyanin that is composed of two identical dodecamers, an allosteric unit size of 8 was determined upon analysis of the oxygen binding data with the simple two-state model. Although $t_D/n = 24/8 = 3$ is an integer implying a trimer of independent 8-mers, this result has no relationship to the structure of the arthropod hemocyanin and is therefore ruled out. When the allosteric unit size was fixed to structurally meaningful values of 6, 12, or 24, an adequate fit was not obtained. Thus a more extended allosteric model was invoked to describe the data with allosteric unit sizes that reflected the structural features of that arthropod protein (Robert et al., 1987; Decker et al., 1988).

The functional characteristics of the *Octopus* system determined by the procedures reported here do not warrant any departure from the most basic two-state allosteric description. Thus our expectation of nested allosteric interaction for this complex system was not found. It may be fortuitous that a single allosteric level with seven equivalent sites fits the data. This implies the involvement of the seven sites of the subunit chain as the allosteric unit. However, a constellation of seven sites taken from several chains may as well be the underlying functional unit.

One may also extend the simple two-state allosteric model to allow for heterogeneity within each allosteric form. Motivation for doing so comes from the heterogeneity observed when the isolated subunit is examined (Miller, 1985; also see Discussion below). When two types of binding sites are allowed for within each allosteric form, the fit did not improve significantly.

Cooperativity, Linkage, and Partitioning of O_2 and CO for the Decamer. The reduced binding capacity is a direct measure of the cooperativity involved in a binding process and is given by the slope of the binding curve; i.e., $\mathbb{B}^*_y = (\partial\theta_x/\partial \ln x)_y$. It is directly related to the slope of the Hill plot, another more routinely used measure of the cooperativity [the Hill slope $n_H = (\partial\theta/\partial \ln a)/[\theta(1-\theta)]$, where θ is the fraction of ligand saturation and a is the activity of the ligand, x or y, for oxygen and carbon monoxide, respectively]. As seen from the plots in Figures 5 and 6, the reduced binding capacity and the Hill slope of oxygen are greatest when no carbon monoxide is present and decrease uniformly with increasing amounts of CO. In terms of the allosteric model, carbon monoxide pulls the equilibrium toward the T state. Since each state alone binds noncooperatively, the oxygen binding capacity will tend toward that for a noncooperative system as the activity of carbon monoxide is increased. On the other hand, carbon monoxide binds nearly noncooperatively in the absence of oxygen, but exhibits a definite positive cooperativity at high partial pressures of oxygen. In terms of the allosteric model, this is accounted for by the ability of oxygen to shift the populations of allosteric states in favor of the R state. In the absence of oxygen, carbon monoxide remains in the T state throughout most of the saturation range.

The competition between carbon monoxide and oxygen in binding to the hemocyanin is clearly demonstrated by the linkage surface in Figure 7. This surface is negative everywhere, except at the asymptotes where it vanishes, because the ligands bind competitively at the same site. The graphical representation of the functional properties of the macromolecule in terms of ligand chemical potentials was suggested by Wyman (1984) in his discussion of linkage graphs. As we have seen, these surfaces provide a direct means to assess the response of the hemocyanin macromolecule to changes in the ligand activities of its environment.

A further comparison of the linked-binding properties of the two ligands is shown by the nonuniform nature of the partition coefficient surface (Figure 8). The strong shape and symmetry disparities in the binding curves for the individual ligands are evidenced by the highly curved partition coefficient surface. The value of the partition coefficient is greatest at low saturations of both ligands, where the molecule is in the T state. As the hemocyanin undergoes the transition to the R state upon binding oxygen, the partition coefficient decreases. Its minimum value occurs at high partial pressures of oxygen and low partial pressures of carbon monoxide where the molecule is largely in the R state.

Linkage and Protons and Heat with Oxygen Binding. Miller (1985) demonstrated that the overall Bohr effect of the *Octopus* decamer was nearly identical at 10 and 20°C. The results reported here at 25 °C are consistent with this observation, indicating an overall temperature-independent Bohr effect. Although the *overall* number of protons released does not change appreciably with temperature, the number of protons released as a function of oxygen saturation varies with both temperature and pH. We may obtain an estimate of the proton release from the horizontal distance between closely spaced binding curves at different pH's at a particular level of saturation, divided by the difference in pH (Wyman, 1984). At a pH of roughly 7.1 (20 °C), the number of protons released at 10% oxygen saturation is 0.45 per mole of oxygen bound. At 90% oxygen saturation there are 2.1 mol of protons released per mole of oxygen bound. At a pH of 7.85, the number of protons released at 10% oxygen saturation is 1.9 and at 90% is 0.9. [These calculations were performed from binding curves generated from the oxygen binding constants obtained by fitting the data of Miller (1985) (Zhou et al.,

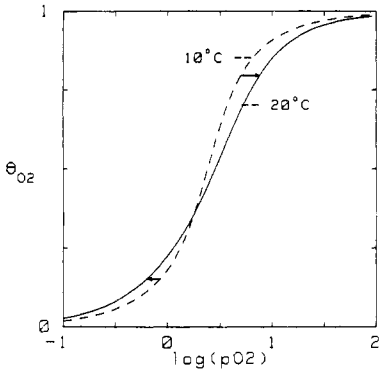

FIGURE 11: Binding curves for decameric *Octopus* hemocyanin at pH 8.00 for T = 10 and 20 °C. The change in the direction of the arrows points out the oxygen reaction is endothermic at low oxygen saturation and exothermic at high oxygen saturation. The curves were generated from the binding constants reported by Zhou et al. (1988).

1988).] Although the sign of the Bohr effect is the same under a range of reported conditions, the relative magnitude of the effect clearly depends upon oxygen saturation. In contrast, the Bohr effect in human hemoglobin is nearly constant over a wide range of oxygen saturation, so that the binding curves at different pH's are nearly parallel (DiCera et al., 1988a).

Just as the number of protons absorbed or released at a particular oxygen saturation may be estimated from oxygen binding curves performed at different pH's, the amount of heat absorbed or released may be estimated from binding curves performed at different temperatures. The relevant linkage relation is $(\partial \Delta H/\partial \bar{X})_T = R(\partial \ln x/\partial T)_{\bar{X}}$, where ΔH is heat of oxygen binding. Thus the change in heat with oxygen saturation may be approximated again by a finite difference between binding curves at a particular level of saturation: $[-2.303R(\Delta \log x)]/(\Delta \log T)$. From the fitted constants reported by Zhou et al. (1988) we generated the binding curves for pH 8.00 at 10 and 20 °C (Figure 11). The striking result is that the two binding curves cross. Thus at low oxygen saturation heat is absorbed and at high saturation heat is released upon oxygen binding. For example, at 15° saturation, ΔH = 5.1 kcal per mole of oxygen bound whereas at 85% saturation, ΔH = −7.6 kcal per mole of oxygen bound. The *overall* enthalpy of the reaction at pH 8.00 is barely exothermic, −0.8 kcal/mol of O_2. This phenomenon was also noted for carbon monoxide binding to trout I hemoglobin (Barisas & Gill, 1979) and was suggested there to confer favorable oxygen delivery at lower temperatures.

Functional Heterogeneity within the Isolated Chain. Since the cooperativity of the decamer might be due to an allosteric cluster based on the subunit chain with seven sites, it is of interest to determine the binding properties of isolated subunits. Miller (1985) reported on the oxygen binding to the isolated chains and concluded from the slopes of Hill plots that no positive cooperativity was present. Furthermore, regions of the Hill plots produced slopes of less than 1, suggesting that there are different classes of binding sites. By analyzing the binding of oxygen and carbon monoxide within the framework of a model that assumes two different types of binding sites, we were able to determine the affinities and numbers of the different types of binding sites.

The number of sites of one type is w and of the other type, $t_c - w$. The value of t_c is known from previous structural studies (Lamy et al., 1987). In the initial fit, w was treated as a variable parameter. The closest integer to the value obtained upon convergence was 4, so that, in the final analysis, the value of w was fixed to 4. As a check, the value of w was fixed to the other possible integral values (1–7). The best fit was obtained with w = 4, meaning that the numbers of sites with affinities of type 1 and type 2 are 4 and 3, respectively. The relative amount of functional heterogeneity found here for *O. dofleini* hemocyanin chains is 4/7 and 3/7 or 57% and 43%, as also found for *Octopus vulgarus* hemocyanin (Zolla et al., 1985).

By examination of the values of the constants reported in Table I, it is evident that the hemocyanin chain exhibits greater functional heterogeneity for oxygen than for carbon monoxide. This effect was noticed in similar studies performed on the chains isolated from other molluscan hemocyanins (Zolla et al., 1985) and may arise from the differences in the mode of binding of the two ligands. Oxygen bridges the two coppers in the binding site whereas CO binds to only one of the coppers (Freedman et al., 1976).

In light of recent work of Miller et al. (1988), the position of one of the low-affinity sites within the chain appears to be at the C-terminal end of the chain. In that study, the C-terminal functional unit (termed the Od 1 fragment), corresponding to one of the "beads" on the isolated chain, was cleaved off and purified. Moreover, it was demonstrated that this isolated functional unit binds oxygen reversibly and that there is a definite Bohr effect. The affinity of this functional unit at pH 8 is 0.017 $Torr^{-1}$, quite close to the value (0.014 $Torr^{-1}$) of the type 1 oxygen binding sites of the chain reported here under similar conditions. In addition, the Hill plots of oxygen binding to the isolated chains at two different pH's show that the asymptotes for the two plots at low oxygen activity are identical, whereas the asymptotes at high oxygen activity are well separated (Miller et al., 1985). This suggests that each class of sites has a different Bohr effect. However, a fuller characterization of the Bohr effects for the chain and isolated fragments is necessary to delineate the situation.

To explore the heterogeneity of binding of the two ligands for the chain and to compare the binding properties of the decamers and isolated chains, reduced binding capacity and linkage property surfaces for oxygen and carbon monoxide are shown in Figure 10. The greater heterogeneity of oxygen binding is seen upon comparing the oxygen binding capacity at very low carbon monoxide activity (essentially the pure oxygen binding capacity) with the carbon monoxide binding capacity at very low oxygen activity. The former is strongly asymmetric whereas the latter is nearly as symmetrical as predicted for simple statistical binding in the absence of heterogeneity. Stronger heterogeneity of carbon monoxide binding is realized at higher activities of oxygen. The linkage property surface for the chain, just as in the decamer, is everywhere negative, but it is much broader, due to the lack of positive cooperativity, than the linkage surface of the decamer shown in Figure 7.

A general comparison of relative ligand affinities for *Octopus* hemocyanin can be made through the magnitude of the partition coefficient. The partition coefficients of arthropod hemocyanins tend to be much smaller than those for the molluscs due to the lower carbon monoxide affinities that arthropod hemocyanins have (Brunori et al., 1981). We note in Table I that the partition coefficients of the decamer and the isolated chain are all greater than 1, as is typically found for molluscan hemocyanins. This supports the notion that there are differences in the structure of the binding site for proteins from the two phyla, a hypothesis that finds support from recent sequence comparisons of arthropod and molluscan hemocyanins (Lang, 1988; Drexel et al., 1987).

The Functional Chemistry of Octopus Hemocyanin. The simple allosteric model, which was found adequate to describe

the cooperativity and linkage properties of oxygen and carbon monoxide, assumes a cluster of seven binding sites, functioning independently, with affinities specified by two allosteric forms within the decameric assembly. In view of the absence of a higher level of nested interaction involving larger allosteric clusters, one naturally wonders why nature has chosen such a highly aggregated structure to serve as the biologically active form of this protein. Clearly, the aggregated assembly of the protein is neccessary to confer the allosteric integrity responsible for cooperative binding. From the complexity of the structure (Van Holde & Van Bruggen, 1971; Lamy et al., 1987) there is no obvious cluster of sites coming soley from the 7-mer subunit chains. Indeed cluster formations involving sites from several chains might be imagined.

In order to create cooperative units, a complex assembly is required, and the stability of the assembled structure becomes paramount for the ultimate functionality of the molecule. Thus one reason for the large size of the native molecule may be to provide sufficient stabilizing interactions between the subunits. This argument has been made for the preservation of the functional integrity and maintenance of the native structures of many proteins due to polysteric forces, i.e., aggregation processes (Robert et al., 1989). In the cases of tarantula and lobster hemocyanins it appears that, in addition to the stability lent by the formation of a macromolecular assembly, there is the ability to fine tune the allosteric control rendered through strong subunit interactions. This is manifested by the presence of a functional hierarchy of control which is deeply rooted in the structure of these proteins and which is embodied by a concept known as nesting (Wyman, 1984; Robert et al., 1987). In the case of the molluscan hemocyanin examined here, the benefits reaped by the formation of a decameric structure lead to a simpler type of control in which the clusters function independently. The maintenance of a multisubunit hemocyanin structure may be just one example of a common mechanism used to ensure the functional integrity of macromolecules. Anthropomorphically speaking, there is strength in numbers.

Registry No. O_2, 7782-44-7; CO, 630-08-0.

References

Barisas, G., & Gill, S. J. (1979) *Biophys. Chem. 9*, 235–244.

Bevington, P. R. (1969) *Data Analysis and Data Reduction in the Physical Sciences*, p 236, McGraw-Hill, New York.

Bonaventura, C., Sullivan, B., Boneventura, J., & Bourne, S. (1974) *Biochemistry 13*, 4784–4789.

Brunori, M., Zolla, L., Kuiper, H. S., & Argo, A. F. (1981) *J. Mol. Biol. 153*, 1111–1123.

Decker, H., Robert, C. H., & Gill, S. J. (1986) in *Invertebrate Oxygen Carriers* (Linzen, B., Ed.) pp 383–388, Springer-Verlag, Berlin and Heidelberg.

Decker, H., Connelly, P. R., Robert, C. H., & Gill, S. J. (1988) *Biochemistry 27*, 6901–6908.

DiCera, E., Doyle, M., Connelly, P., & Gill, S. J. (1987a) *Biochemistry 26*, 6494–6502.

DiCera, E., Wyman, J., & Gill, S. J. (1987b) *Proc. Natl. Acad. Sci. U.S.A. 89*, 449–452.

DiCera, E., Doyle, M., & Gill, S. J. (1988a) *J. Mol. Biol. 200*, 593–599.

Di Cera, E., Gill, S. J., & Wyman, J. (1988b) *Proc. Natl. Acad. Sci. U.S.A. 85*, 449–452.

Dolman, D., & Gill, S. J. (1978) *Anal. Biochem. 87*, 127–134.

Drexel, R., Siegmund, S., Schneider, H., Linzen, B., Gielens, C., Preux, G., Lontie, R., Kellerman, J., & Lottspeich, F. (1987) *Biol. Chem. Hoppe-Seyler 368*, 617–635.

Freedman, T. B., Loehr, J. S., & Loehr, T. M. (1976) *J. Am. Chem. Soc. 98*, 2809–2815.

Haldane, J. S., & Smith, J. L. (1987) *J. Physiol. (London) 22*, 231–258.

Lamy, J., Leclerc, M., Sizaret, P., Lamy, J., Miller, K., McPharland, R., & Van Holde, K. (1987) *Biochemistry 26*, 3509–3518.

Lang, W. H. (1988) *Biochemistry 27*, 7276–7282.

Miller, K. (1985) *Biochemistry 24*, 4582–4586.

Miller, K., & Van Holde, K. E. (1982) *Q. Rev. Biophys. 15*, 1–70.

Miller, K., Van Holde, K. E., Toumadje, A., Johnson, W. C., & Lamy, J. (1988) *Biochemistry 27*, 7282–7288.

Monod, J., Wyman, J., & Changeux, J. P. (1965) *J. Mol. Biol. 12*, 88–112.

Potts, W. J. W., & Todd, M. (1965) *Comp. Biochem. Physiol. 16*, 479.

Ratkowsky, D. A. (1983) *Nonlinear Regression Modeling*, pp 15–17, Marcel Dekker, New York.

Richey, B., Decker, H., & Gill, S. J. (1985) *Biochemistry 24*, 109–117.

Robert, C. H., Decker, H., Richey, B., Gill, S. J., & Wyman, J. (1987) *Proc. Natl. Acad. Sci. U.S.A. 84*, 1891–1895.

Robert, C. H., Colisimo, A., & Gill, S. J. (1989) *Biopolymers* (in press).

Van Holde, K. E., & Van Bruggen, E. F. J. (1971) in *Subunits in Biological Systems* (Timasheff, S. N., & Fasmen, G. D., Eds.) pp 1–53, Marcel Dekker, New York.

Van Holde, K. E., & Miller, K. (1985) *Biochemistry 24*, 4577–4582.

Wyman, J. (1948) *Adv. Protein Chem. 4*, 407–531.

Wyman, J. (1964) *Adv. Protein Chem. 19*, 223–286.

Wyman, J. (1984) *Q. Rev. Biophys. 17*, 453–488.

Zhou, G., Ho, P. S., & Van Holde, K. E. (1988) *Biophys. J.* (in press).

Zolla, L., Brunori, M., Richey, B., & Gill, S. J. (1985) *Biophys. Chem. 22*, 271–280.